Phys. Status Solidi C **6**, No. 5, 1332–1335 (2009) / **DOI** 10.1002/pssc.200881181

physica status solidi c

www.pss-c.com

current topics in solid state physics

Mechanisms of hopping conductivity of p-CdSb:Ni in magnetic field

R. Laiho[1], A. V. Lashkul[1, 2], K. G. Lisunov[1, 2, 3], E. Lähderanta[*, 2], M. A. Shakhov[1, 4], and V. S. Zakhvalinskii[1, 5]

[1] Wihuri Physical Laboratory, University of Turku, 20014 Turku, Finland
[2] Department of Mathematics and Physics, Lappeenranta University of Technology, 53851 Lappeenranta, Finland
[3] Institute of Applied Physics ASM, Academiei Str. 5, 2028 Kishinev, Moldova
[4] A. F. Ioffe Physico-Technical Institute, 194021 St. Petersburg, Russia
[5] Department of Physics, Belgorod State University, 308015 Belgorod, Russia

Received 1 September 2008, revised 29 October 2008, accepted 2 November 2008
Published online 25 February 2009

PACS 72.20.Ee, 72.20.My, 72.25.Dc, 75.50.Pp, 75.50.Tt

[*] Corresponding author: e-mail lahderan@lut.fi, Phone: +358 5 621 6800, Fax: +358 5 621 289

Hopping conductivity in single crystals of the group II-V anisotropic diluted magnetic semiconductor p-CdSb:Ni, oriented along the [100] (# 1), [010] (# 2) and [001] (# 3) axes, is investigated in zero and pulsed magnetic fields B. At $B = 0$ the Mott variable-range hopping (VRH) conductivity is observed in # 2, and the Shklovskii-Efros VRH conductivity in # 1 and # 3 at $T \leq 2.5$ K. However, in weak fields of $B < 6$ T temperature dependence of the resistivity gives evidence for the Mott VRH conductivity in # 1 below ~ 4.2 K, whereas in # 2 and # 3 the nearest-neighbour hopping (NNH) conductivity is observed between 3–4.2 K and between 1.5–4.2 K, respectively. Eventually, in high magnetic fields of B up to ~ 15 T and $T \leq$ 4.2 K only the NNH conductivity is observed in all investigated samples. The analysis of the resistivity data yields the set of microscopic parameters, such as the localization radius, the widths of the Coulomb gap and of the impurity band, the density of the localized states and the anisotropy coefficients, as well as the values of the acceptor concentration and the dielectric permittivity.

1 Introduction A group II-V orthorhombic semiconductor CdSb has attracted attention due to its strongly anisotropic transport properties [1]. In addition, CdSb weakly doped with Ni (p-CdSb:Ni), demonstrates large anisotropy of magnetic properties, accompanied with spin-freezing phenomena already below the room temperature [2]. Such behavior is connected to presence of an assembly of Ni-rich $Ni_{1-x}Sb_x$ magnetic nanoclusters, having a broad size distribution, large non-sphericity and orientations distributed along a preferred direction [2]. This makes p-CdSb:Ni a promising new diluted magnetic semiconductor.

In this work we investigate resistivity and magnetoresistance (MR) of p-CdSb:Ni to obtain information about mechanisms of the low-temperature hopping charge transfer and microscopic parameters of charge carriers.

2 Results and discussion Single crystals of CdSb doped with 2 at.% of Ni were prepared with the modified Bridgman method [1, 2]. Samples with a form of rectangular prisms with longest edge along the [100] (# 1), [010] (# 2) and [001] (# 3) axes, respectively, were cut from the ingots for investigations. The measurements of the resistivity, ρ, were made between T = 1.5–300 K in zero magnetic field, B, or in pulsed fields up to B = 30 T, in transversal configurations with j || [100] and B || [001] (# 1), j || [010] and B || [100] (# 2), j || [001] and B || [010] (# 3), where j and B are the vectors of the current density and the magnetic induction, respectively.

As can be seen from the top panel of Fig. 1 the resistivity at $B = 0$ has two intervals of the activated behavior, characterized by different slopes. The first one (between ~ 5–20 K) is connected to activation of holes from acceptor band (AB) into the valence band (VB), yielding the activation energies E_A = 2.45, 2.50 and 2.85 meV for # 1, # 2 and # 3, respectively. The second slope (below $T \approx$ 2.5 K) is connected to the variable-range hopping (VRH) charge

transfer over localized states of the AB. Indeed, the hopping resistivity satisfies the general expression $\rho\ (T) = AT^{m} \times \exp\ [(T_0/T)^{p}]$ [3], A is a constant, $m = p$ as predicted for doped semiconductors with shallow impurities and hydrogenic wave functions (the meaning of p is clarified below), and T_0 is the characteristic temperature [3]. In the regime of nearest-neighbor hopping (NNH) $p = 1$ and $T_0 = E_n / k_B$, where E_n is the NNH activation energy and k_B is the Bolzmann constant. For the Mott VRH we have $p = 1/4$ and $T_0 = T_{0M}$, whereas for the Shklovskii-Efros (SE) VRH regime $p = 1/2$ and $T_0 = T_{0SE}$ [3]. The SE VRH conductivity sets in due to microscopic disorder and Coulomb interaction between the charge carriers leading to appearance of Coulomb gap, Δ, in the spectrum of the density of localized states (DOS) with width W, having the optimal observation when Δ and W are comparable. The Mott VRH conductivity takes place as far as the Coulomb interaction between the carriers can be neglected, with condition of $\Delta << W$ being preferable for observation. The regime of hopping can be established by analyzing the local activation energy, $E_a \equiv d\ ln\ \rho / d\ (k_B T)^{-1}$ [3]. Taking into account the expression for $\rho\ (T)$ above we obtain: $\ln\ [\ E_a/(k_B T) + m] = \ln p + p\ \ln T_0 + p\ \ln (1/T)$, yielding the value of p at a given m as the slope of the plots in the bottom panel of Fig. 1. One can see from this figure that the SE VRH conductivity takes place in # 1 and # 3 (where p is close to 1/2), whereas in # 2 the Mott VRH conductivity (with $p \approx 1/4$) is observed. The parameters T_{0M} and T_{0SE} have been found from the plots of $\ln\ (\rho/T^{m})$ vs. T^{-p} (not shown), yielding the values of T_{0SE} = 18.7 K (# 1), T_{0M} = 3180 K (# 2) and T_{0SE} = 51.3 K (# 3).

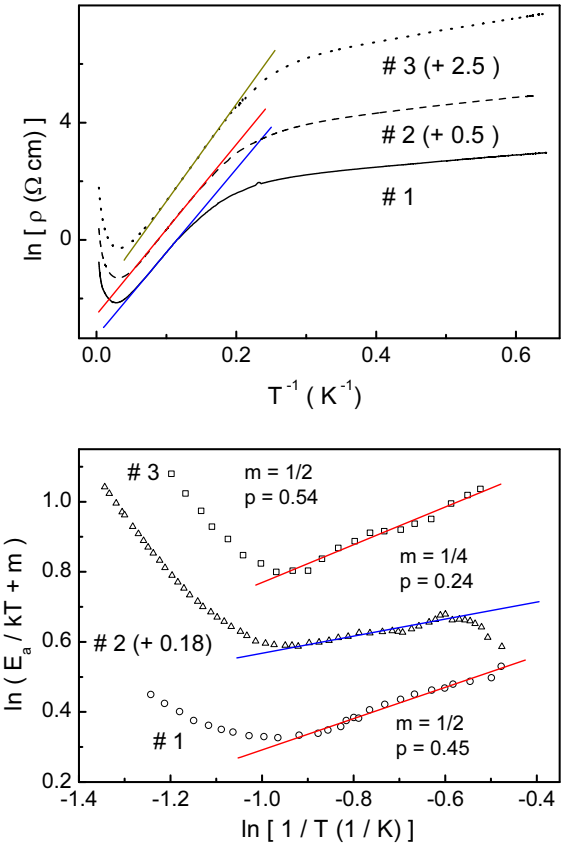

Figure 1 Plots of ln ρ vs. T^{-1} (top panel) and of ln (E_a/kT + m) vs. ln (1/T) (bottom panel) in the investigated samples at B = 0. The lines are linear fits.

The positive MR is observed in p-CdSb:Ni at any T and B used in our experiments. It will be analyzed below at temperatures corresponding to hopping conduction, separately in the intervals of weak and strong fields, where the dependence of ρ on B is predicted to be different [3].

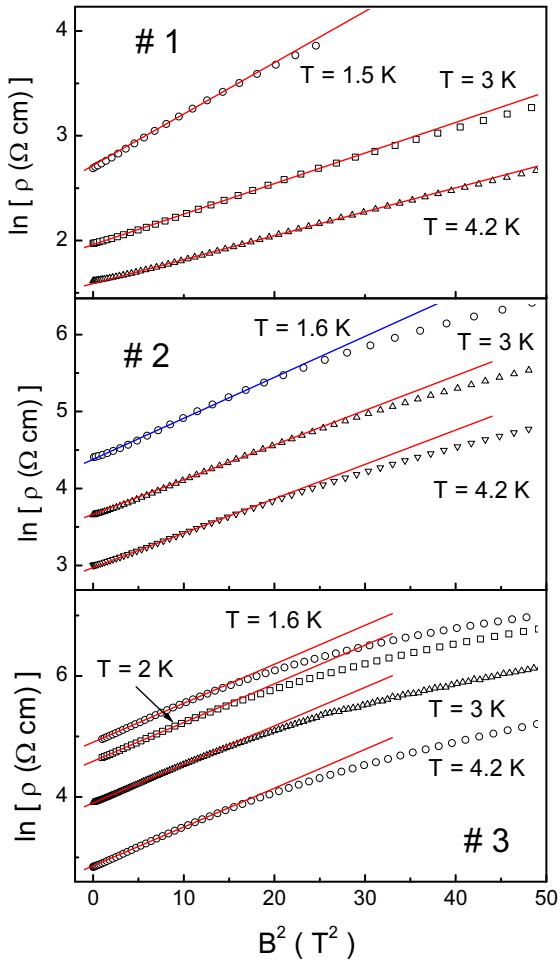

Figure 2 Plots of ln ρ vs. B^2 for the investigated samples. The lines are linear fits to the experimental data.

As follows from Fig. 2 the plots of ln ρ vs. B^2 in low fields of B < 6 T can be approximated well with linear functions. In # 3 the slope of the plots is constant between 1.6–4.2 K. The slope of the corresponding plots for # 2 does not vary between 3–4.2 K and increases only slightly between 3–1.6 K. In sample # 1 all the plots have different slopes varying with temperature.

Quadratic dependence of ln ρ on B in weak fields has been predicted for any mechanism of the hopping conduc-

tivity, taking into account shrinkage of impurity wave functions by the magnetic field [3]. However, the dependence of ln ρ (B) on temperature is different for each hopping regime. The law $\ln[\rho(B)/\rho(0)]_j = C_j B^2$ is expected for the NNH conductivity, where $C_j = t\, e^2\, a\, p_j^2/(\hbar^2\, N_A)$ does not depend on T, $t = 0.036$, e is the elementary charge, a is the mean localization radius, $p_j = [m_j^2/(m_k m_l)]^{1/6}$ is the anisotropy coefficient (m_j, m_k and m_l are the components of the hole effective mass), with j, k, $l = 1, 2, 3$ ($j \neq k \neq l$) and $j = 3, 1, 2$ for # 1, # 2 and # 3, respectively, corresponding to the direction of the *magnetic field* along the [001], [100] and [010] axes, respectively, ħ is the Planck constant and N_A is the acceptor concentration [3, 4]. For the Mott-VRH conductivity in low fields one gets an expression similar to that of the NNH conductivity, but with C_j replaced by $A_j^{(M)}(T) = A_{0j}^{(M)}\, T^{-3/4}$, where $A_{0j}^{(M)} = t_1 e^2\, a^4\, T_{0M}^{3/4}\, p_j^2 / \hbar^2$ and $t_1 = 5/2016$ [3]. Finally, for the SE-VRH conductivity in low fields, instead of C_j we have $A_j^{(SE)}(T) = A_{0j}^{(SE)}\, T^{-3/2}$, where $A_{0j}^{(SE)}$ is given by an expression similar to $A_j^{(M)}(T)$, but with $t_2 = 0.0015$ and T_{0SE} instead of t_1 and T_{0M}, respectively [3].

From comparison of the behavior of the experimental slopes of the plots of ln ρ vs. B^2 in Fig. 2 with C_j, $A_j^{(M)}(T)$ and $A_j^{(SE)}(T)$, predicted for the different hopping regimes (see above), it follows that contrary to the case of $B = 0$, in # 1 the Mott VRH conductivity takes place between 1.6 – 4.2 K, whereas in # 2 and # 3 the NNH conductivity is observed between 3–4.2 and 1.6–4.2 K, respectively.

Using the values of T_{0SE} and T_{0M} obtained above, the expressions for them, $T_{0M} = \beta_M/[k_B\, g(\mu) a^3]$ and $T_{0SE} = \beta_{SE} e^2/(k_B\, \kappa\, a)$, respectively (where $\beta_M = 21$, $\beta_{SE} = 2.8$ and κ is the dielectric permittivity) [3], the values of the slopes of the plots in Fig. 2, as well as the equations for critical behavior of a and κ near the metal-insulator transition (MIT), $a = a_0(1–N_A/N_C)^{\nu}$ and $\kappa = \kappa_0(1–N_A/N_C)^{-\zeta}$, respectively (where N_C is the critical acceptor concentration corresponding to MIT, a_0 and κ_0 are the values of a and κ far from MIT, ν and ζ are the critical exponents), a set of microscopic parameters of the charge carriers have been determined. We obtained a = 196, 180 and 139 Å, Δ = 0.30, 0.18 and 0.49 meV, W = 0.50, 1.28 and 0.91 meV, and DOS outside the Coulomb gap g = 5.94, 1.31 and 2.16 (in units of 10^{16} cm^{-3} meV^{-1}) for # 1, # 2 and # 3, respectively. In addition, the values of N_A = 3.61, 3.37 and 2.51 (in units of 10^{16} cm^{-3}), κ = 127, 108 and 66, p_j = 0.839 (0.839), 1.008 (0.897) and 1.182 (1.327) have been found (in parenthesis are given the corresponding calculated values with m_i taken from [4]) for # 1, # 2 and # 3, respectively, as well as $N_C = 6.275\times10^{16}$ cm^{-3}, ν = 1.00 and ζ = 1.90.

One can see that ν and ζ are close to their theoretical values (1 and 2, respectively) [5], the values of N_A in all samples are rather close to N_C, in agreement with the behavior of the parameters a and κ exceeding those of a_0 = 83.5 Å (evaluated with the values of E_A and m_i [4] according to [3]) and $\kappa_0 = 25$ [6], the anisotropy coefficients p_j are close to the calculated values $p_j^{(cal)}$, and Δ is comparable with W in # 1, 3 and $\Delta << W$ in # 2, in agreement with observations of the SE-VRH conductivity in # 1, 3 and the Mott-VRH conductivity in # 2 (Fig. 1). At this point, transition to the SE VRH in # 2 is expected below $T_v' \approx 0.7$ K, with the low-temperature downturn of the plot of $\ln(E_a/k_B\, T + m)$ vs. ln $(1/T)$ for this sample being attributable to intermediate interval between the Mott and SE VRH conductivity regimes. Hence, the (joint) analysis of the resistivity in zero and weak fields yields a consistent picture with reasonable values of the parameters determined above. It is worth mentioning that both the values of N_A and E_A obtained above are similar to those of undoped p-CdSb [1, 4] suggesting only a small perturbation of the acceptor system in the p-CdSb:Ni samples investigated here. This is in line with negligible variation of the lattice parameters with respect to the values in undoped p-CdSb [1, 2], as well as with inhomogeneous distribution of Ni leading to Ni-rich magnetic clusters as mentioned in the Introduction [2].

In strong magnetic fields the positive MR is connected to shrinkage of the impurity wave functions by the field, too, accompanied with the magnetic field dependence of both a_0 (B) and E_A (B) with the onset defined by condition of $\lambda \sim a_0$ (0), where λ is the magnetic length [3]. In the NNH conductivity regime MR is given by the equation

$$\ln [\rho\,(B) / \rho^*]_j = \eta_j [\, B\, \varphi\,(B)]^{1/2}, \qquad (1)$$

where ρ* is a constant, $\eta_j = q\, p_j^{1/2}\, [e/(N_A\, a\, \hbar)]^{1/2}$, $q = 0.92$ and $\varphi\,(B) = a/a\,(B)$, yielding $\varphi\,(B) = 1$ if the dependence of a on B is neglected. Far from the MIT we have $\varphi\,(B) \equiv \varphi_0\,(B) = a_0/a_0\,(B)$, where $a_0 \sim E_A^{-1/2}$ [3], so that $\varphi\,(B)$ is determined entirely by $E_A\,(B)$, given by expressions $E_A\,(B) = E_A\,(0) \equiv E_A$ for $B << B_0$ and $E_A\,(B) = E_A \ln^2(B/B_0)$ for $B >> B_0$ [3], $B_0 \equiv \hbar/(e a_0^2)$ being a field where $\lambda = a_0$. In our case of $B_0 = 9.5$ T the interval of high fields (see below) corresponds to $B \sim B_0$ or $\lambda \sim a_0$, where $E_A(B)$ cannot be obtained analytically [3]. On the other hand, this function can be approximated well with the relation $E_A(B) = \beta\, B^{1/3}$, where β is independent of B [3]. The dependence $E_A\,(B)$ was found approximately from the plots of ln ρ (B, T) vs. T^{-1} in the temperature interval of the acceptor freeze-out (examples are shown for # 1 in Fig. 3). Then β is obtained from the plots of E_A vs. $B^{1/3}$ which are close to linear between B = 10–15 T (inset to Fig. 3) yielding the values of β = 1.64, 1.53 and 1.19 meV T$^{-1/3}$, and $\varphi_0(B) = (\beta\, B^{1/3}/E_A)^{1/2}$.

Eventually, in the most general way of non-vanishing magnetic field dependence of a and at arbitrary proximity to the MIT we obtain

$$\varphi(B) \approx \frac{(3/2)(1+\gamma_0)+(1/6)\gamma_0^2}{(3/2)[1+\gamma_0(B)]+(1/6)[\gamma_0(B)]^2} \exp\{-\gamma_0[1-\varphi_0(B)]\}, \qquad (2)$$

where $\gamma_0(B) \equiv R_A/a_0(B)$ and $R_A = (4\pi N_A/3)^{-1/3}$ is half of the mean distance between the acceptors.

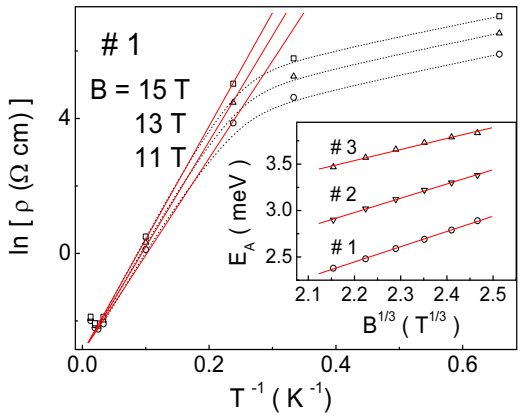

Figure 3 The dependence of ln ρ on T^{-1} for # 1 at B = 15 T, 13 T and 11 T (from up to down). Inset: plots of E_A vs. $B^{1/3}$. The dotted lines are guides for the eye and the solid lines are linear fits.

As can be seen from Fig. 4 the plots of ln ρ vs. $[B\ \varphi\ (B)]^{1/2}$ exhibit linear behavior in the interval of B between ~ 4–15 T, and their slopes do not depend on temperature at $T \leq 4.2$ K in # 1 and # 2 and between 3 – 4.2 K in # 3, in agreement with Eq. (1). The values of the slopes $\eta^{(ex)}$ obtained from the plots in Fig. 4, $\eta^{(ex)}$ = 1.36, 1.50 and 2.00 $T^{-1/2}$ for # 1, # 2 and # 3, respectively, exhibit a good agreement with the calculated values, $\eta_j^{(cal)}$ = 1.23, 1.46 and 2.09 $T^{-1/2}$ for # 1, # 2 and # 3, respectively. Hence, the behavior of MR in p-CdSb:Ni in the interval of B between ~ 4–15 T is governed by the NNH conductivity in the limit of strong fields, excluding lowest T in # 3, where, however, MR does not agree with any other hopping model for conventional semiconductors requiring increase of the slopes of the plots like those in Fig. 4 with decreasing temperature. Deviation of all the plots in Fig. 4 from linearity with increasing B is attributable to the onset of the logarithmic asymptote of E_A (B) (see above).

Finally, one can see a tendency of changing the VRH conductivity, observed at B = 0, into the NNH conductivity with increasing magnetic field, which is uncommon in conventional (non-magnetic) semiconductors. However, in p-CdSb:Ni such tendency is in line with damping of the internal magnetic disorder, connected to presence of magnetic nanoclusters (see Introduction) by aligning their moments in a field (which takes place already at B ~ 4 kG [2]) and reducing the potential barriers between different acceptor sites, which stimulates transitions between nearest neighbors leading to NNH when B is increased.

3 Conclusions We have investigated mechanisms of hopping conductivity of p-CdSb:Ni in zero and pulsed magnetic fields up to 30 T. Analysis of the resistivity and MR data yielded the values of the microscopic parameters of charge carriers, as well as the dielectric permittivity and the acceptor concentration.

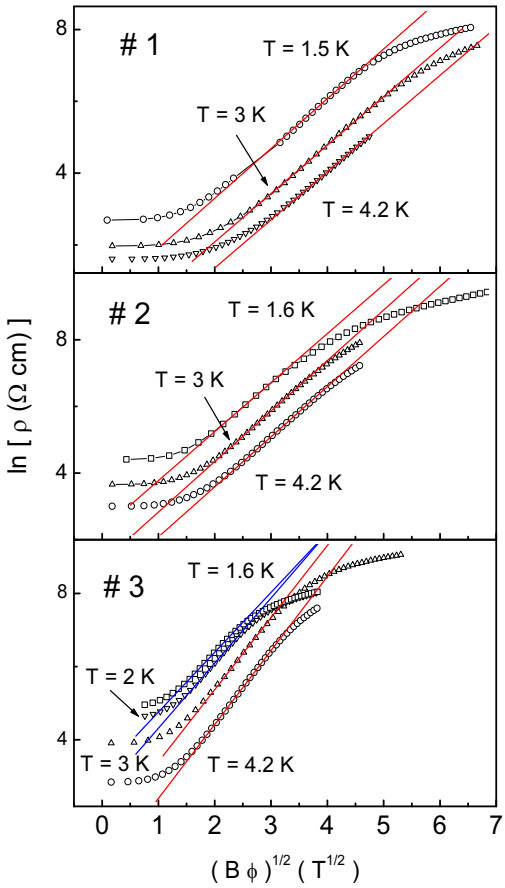

Figure 4 Plots of ln ρ vs. $(B\varphi)^{1/2}$. The lines are linear fits.

References

[1] E. K. Arushanov, Prog. Cryst. Growth Charact. **13**, 1 (1986).
[2] R. Laiho, A. V. Lashkul, K. G. Lisunov, E. Lähderanta, I. Ojala, and V. S. Zakhvalinskii, Semicond. Sci. Technol. **21**, 228 (2006).
[3] B. I. Shklovskii and A. L. Efros, Electronic Properties of Doped Semiconductors (Springer, Berlin, 1984).
[4] R. Laiho, A. V. Lashkul, K. G. Lisunov, E. Lähderanta, M. O. Safonchik, and M. A. Shakhov, J. Phys.: Condens. Matter **16**, 333 (2004).
[5] T. G. Castner, in: Hopping Transport in Solids, edited by M. Pollak and B. Shklovskii (Elsevier, Amsterdam, 1991), ch. 1.
[6] A. M. Borets, I. M. Rarenko, and V. V. Rusnak, in: Proceedings of the 6th All-Union Joint Conference on Materials Science of II-V Semiconductors, Kamenetsk-Podol'skii, USSR, 1984 (IONH, Moscow, 1984), p. 108.